https://doi.org/10.5194/acp-2022-549
Preprint. Discussion started: 17 October 2022

Atmospheric Chemistry and Physics Discussions

Global warming will largely increase CH_4 emissions from waste treatment: insight from the first city scale CH_4 concentration observation network in Hangzhou city, China

Cheng Hu[1,2], Junqing Zhang[1], Bing Qi[3,4*], Rongguang Du[3]*, Xiaofei Xu[4], Haoyu Xiong[5], Huili Liu[1], Xinyue Ai[1], Yiyi Peng[1], Wei Xiao[2]

[1] College of Biology and the Environment, Joint Center for sustainable Forestry in Southern China, Nanjing Forestry University, Nanjing 210037, China

[2] Collaborative Innovation Center on Forecast and Evaluation of Meteorological Disasters (CIC-FEMD), Nanjing University of Information Science & Technology, Nanjing, China

[3] Hangzhou meteorological bureau, Hangzhou 310051, China

[4] Zhejiang Lin'an Atmospheric Background National Observation and Research Station, Hangzhou 311300, China

[5] College of Environment, Zhejiang University of Technology, Hangzhou 311300, China

*Corresponding authors: Bing Qi (bill_129@sina.com), Rongguang Du (drg1998@163.com).

https://doi.org/10.5194/acp-2022-549
Preprint. Discussion started: 17 October 2022

Atmospheric Chemistry and Physics Discussions

Abstract:

Atmospheric CH_4 is the second largest anthropogenic contributor to global warming, however its emissions, components, spatiotemporal variations, and projected changes present large uncertainties from city to national scales. CH_4 emissions from waste treatment account for >50% of total anthropogenic CH_4 emissions at the city scale, and considering the high sensitivity of CH_4 emission factors (EFs) to temperature for biological process-based sources, such as waste treatment, large bias will occur when estimating future CH_4 emissions under different global warming scenarios. Furthermore, the relationships between temperature and waste treatment CH_4 emissions have only been determinized in a few site-specific studies, and these findings lack representativeness for the whole city scale, which contains various biophysical conditions and shows heterogeneous distribution. These factors increase the difficulty of evaluating city-scale CH_4 emissions (especially from waste treatments), and the projected changes remain unexplored. Here, we conduct the first tower-based CH_4 observation network with three sites in Hangzhou city, which is located in the developed Yangtze River Delta (YRD) area and ranks as one of the largest megacities in China. We found that the *a priori* total annual anthropogenic CH_4 emissions and waste treatment emissions were overestimated by 36.0% and 47.1% in Hangzhou city, respectively. However, the total emissions in the larger region of Zhejiang Province or the YRD area was only slightly underestimated by 7.0%. Emissions from waste treatment showed obvious seasonal patterns according to the air temperature. By using the constructed linear relationship between monthly waste treatment CH_4 emissions and air temperature, we found that the waste treatment EFs increased by 38%~50% as the temperature increased by 10°C. Together with the projected temperature changes from four climate change scenarios, the global warming-induced EFs in Hangzhou city will increase at rates of 2.2%, 1.2%, 0.7% and 0.5% per decade for RCP8.5, RCP6.0, RCP4.5 and RCP2.6 scenarios, respectively, and by 17.6%, 9.6%, 5.6%, and 4.0% at the end of this century, respectively. Additionally, the relative changes derived for the whole of China also showed high heterogeneity and indicated large uncertainty in projecting future national total CH_4 emissions. Hence, we strongly suggest the temperature-dependent EFs and positive feedback between global warming and CH_4 emissions should be considered in future CH_4 emission projections and climate change models.

Keyword: CH_4 emissions, waste treatment, observation network, global warming

https://doi.org/10.5194/acp-2022-549
Preprint. Discussion started: 17 October 2022

Atmospheric Chemistry and Physics Discussions

1. Introduction

CH_4 is the second largest anthropogenic greenhouse gas, and reducing CH_4 emissions is considered an effective way to mitigate future climate change on short timescales (Henne et al., 2016; Lin et al., 2021). Accurate estimation of CH_4 emissions from main sources represent the basis of policy making. However, recent studies have found that the total emissions, components, spatiotemporal variations, and projected changes still have large uncertainties at the city scale, especially for megacities in China (USPA 2013; Cai et al., 2018; Lin et al., 2021). Waste treatment (mainly sewage and solid waste from landfills and incineration) is ranked as the world's third largest anthropogenic source of CH_4 emissions after fuel exploitation and livestock, and these emissions account for ~13% of global anthropogenic CH_4 emissions of 371 (±26) Tg a^{-1} (Lu et al., 2021). It is also ranked as the fourth largest anthropogenic source in China, the biggest anthropogenic CH_4 emitting country, and accounted for ~14% of the total national anthropogenic emissions of 65 (±22) Tg a^{-1} (Saunois et al., 2020; Lu et al., 2021; Chen et al., 2022). Furthermore, its contribution is larger than 50% at the city scale, where more household waste is located. Therefore, the accurate quantification of waste treatment CH_4 emissions in urban areas has become increasingly important.

Although some progress has been made in measuring site-scale CH_4 emissions from waste treatment, the estimated emissions still show large discrepancies owing to many factors, such as the amount of waste and its composition, meteorological conditions, such as temperature and water content, proportion between landfills and incineration, degradable organic carbon ratio, CH_4 oxidation efficiency, and landfill gas collection (Masuda et al., 2018; Cai et al., 2018; Zhao et al., 2019; Hua et al., 2022; Bian et al., 2022; Maasakkers et al., 2022). Furthermore, CH_4 emissions from sewage and landfills are caused by microbial process, especially methanogens, and their emission factors (EFs) are highly sensitive to temperature. These studies were mainly conducted at specific sites with various reported EFs (Du et al., 2017; 2018; Cai et al., 2014; 2018; Zhao et al., 2019; NBSC, 2015; Wang et al., 2015; Florentino et al., 2010; Tolaymat et al., 2010; Hua et al., 2022). The lack of detailed information for all the above factors and their uncertainties has led to considerable bias in estimating CH_4 emissions for most up-to-date inventories (Höglund-Isaksson,

https://doi.org/10.5194/acp-2022-549
Preprint. Discussion started: 17 October 2022


Atmospheric Chemistry and Physics Discussions

2012; USPA et al., 2013; Cai et al., 2018; Lin et al., 2021; Maasakkers et al., 2022).

China is a developing country with the largest anthropogenic CH_4 emissions, its emissions are expected to increase because of the projected rapid economic development, urbanization, and waste generation (Cai et al., 2018). The increase in waste treatment emissions in East China was also found to be the second largest sector driving national total anthropogenic CH_4 emissions since 2000 (Lin et al., 2021). Moreover, the mitigation potential of waste treatment in developing countries is thought to be four times than in developed countries (USEPA, 2013). Therefore, mitigating CH_4 emissions from waste treatment in China is a robust and cost-effective method of reducing the total national anthropogenic greenhouse gas emissions.

Many previous studies have estimated the waste treatment CH_4 emissions for China by both "bottom-up" and "top-down" approaches, with the results varied by 2.5-fold from 4.3 to 10.4 Tg CH_4 yr^{-1}, and accounted for 8.1%~24.2% of national total anthropogenic CH_4 emissions (USEPA 2013; Peng et al., 2016; Miller et al., 2019; Lin et al., 2021; Lu et al., 2021; Chen et al., 2022). For these "bottom-up" approach, the high uncertainties were directly attributed to the absence of many small point sources and discrepancies of observed site-specific EFs, which varied largely based on the climate and management technology (Zhao et al., 2019; Hua et al., 2022). As found in previous studies, the most commonly used EDGAR (The Emission Database for Global Atmospheric Research) inventory always uses IPCC-recommended default EF values as 15.0% (Höglund-Isaksson, 2012; Lin et al., 2021; Bian et al., 2022); however, this value is approximately 5-7 times of EFs used in China by Zhang and Chen et al. (2014). A recent study comparing waste treatment CH_4 emissions among different inventories also reported that the EDGAR v5.0 and CEDS (Community Emissions Data System) inventories were 21~153% higher than other inventories and EDGAR v5.0 tended to assign more emissions in urban area, especially provincial capitals. In addition, emissions from wastewater have been overestimated by higher emission factor or chemical oxygen demand (Peng et al., 2016; Lin et al., 2021).

For the "top-down" atmospheric inversion approach, a few studies have constrained anthropogenic

https://doi.org/10.5194/acp-2022-549
Preprint. Discussion started: 17 October 2022


Atmospheric Chemistry and Physics Discussions

sources, including waste treatment, where the most widely used concentrations were satellite observations (Miller et al., 2019; Lu et al., 2021; Chen et al., 2022). Satellite retrieval has the advantage of easy access and global coverage. However, as already noted, the emission constraint results were highly dependent on the availability of observed concentrations, which were largely influenced by weather conditions and cloud coverage. As illustrated in a nearly published study by Chen et al. (2022), although the number of grid cell (0.25° ×0.3125°)-based year-round satellite observations was more than 1000 in north China, the available numbers were less than 10 (and even without any observations) in most part of central, western, eastern and southern China. Such a sparse distribution of available data may not provide robust constraints on waste treatment emissions for some Chinese cities without enough observations, especially considering that waste treatment is co-located with high population density megacities in developed areas, such as eastern and southern China. Furthermore, large temperature-induced monthly variations should occur in waste treatment CH_4 emissions; however, almost all satellite-based inversions were conducted at an annual scale without seasonal variations. Only one recent study was based on satellite observations and focused on urban waste treatment CH_4 emissions, and it found that annual total CH_4 emissions from four cities were 1.4 to 2.6 times larger than inventories in India and Pakistan, where landfills contributed to 6~50% of total emissions and indicated a large bias in our understanding of waste treatment CH_4 emissions (Maasakkers et al., 2022).

The tower-based atmospheric inversion approach, which is based on hourly atmospheric concentration observations within the planetary boundary layer, can be used independently to constrain CH_4 emissions and their main components. Compared with “bottom-up” approach, this method can avoid using the factors that lead to large uncertainties of CH_4 emissions, especially from waste treatment. To the best of our knowledge, tower-based observation inversion studies have not focused on waste treatment emissions at the city scale or much larger regional scales, especially in China. In addition, the influences of global warming on city-scale (or higher regional-scale) emissions are still unclear and have not been considered in future emission projections (USEPA 2013; Cai et al., 2018). In general, previous studies that predicted future waste treatment CH_4 emissions only used activity data changes without considering climate

https://doi.org/10.5194/acp-2022-549
Preprint. Discussion started: 17 October 2022


Atmospheric Chemistry and Physics Discussions

change effect on its EFs. Considering the potential high sensitivity of waste treatment CH_4 emissions to projected global warming, how the emissions change with increasing temperature is still unknown, especially within megacities, where more waste is generated and the urban heat island effect will lead to a much stronger warming climate (Zhang et al., 2022).

In this study, we established three tower-based CH_4 concentration observation sites in Hangzhou city, which is one of the largest megacities in China. To the best of our knowledge, this is the first city-scale, tower-based CH_4 concentration observation network in China. We present our work on urban CH_4 emissions inversion and aim to (1) constrain CH_4 emissions from waste treatment alongside total anthropogenic emissions in Hangzhou city and (2) derive the temperature sensitivity of waste treatment CH_4 emissions at the city scale and quantify the projected emission changes in future climate change scenarios. One-year hourly CH_4 concentration observations from December 1, 2020, to November 30, 2021, were combined with the atmospheric transport model and Bayesian inversion approach to constrain the monthly CH_4 emission inventories. The constructed relationship between monthly temperature and *posteriori* waste treatment CH_4 emissions will be used with future temperature projections to quantify how the EFs will change under different global warming scenarios.

2. Materials and Method

2.1 Tower-based CH_4 observation network and supplementary materials

Hangzhou city, which has a population of 12.2 million and an area of 1.7×10^4 km^2 (core urban area of 8.3×10^3 km^2), is the capital of Zhejiang province and located in middle of East China (Figure 1a). As displayed in Figures S1-S2, the East China accounted for the majority of national total population and waste treatment CH_4 emissions, and Hangzhou city ranked among the top 10 megacities in China in terms of waste, with an annual solid waste of around 5 million tons in 2021. The tower-based CH_4 concentration observation network includes three observation sites (Figure 1a-d): (1) Hangzhou site (120.17° E, 30.23° N, 43.2 m a.s.l.), which is located in the core urban regions; (2) Linan site (119.72° E, 30.30° N, 138.6 m a.s.l.), which is located in the regional background with no obvious emission sources within a 10 km radius; (3) Damingshan site

https://doi.org/10.5194/acp-2022-549
Preprint. Discussion started: 17 October 2022


Atmospheric Chemistry and Physics Discussions

(119.00° E, 30.03° N, 1485.0 m a.s.l.), which is located on the top of a 1500 m mountain and represents a background with much more diluted regional emission signals. The distance is around 50 km between Hangzhou and Linan sites and approximately 150 km between the Hangzhou and Damingshan sites. These three sites represent obvious gradients from east, with densely populated areas (Figure 1c-d) and anthropogenic emissions, to the west, with much weaker anthropogenic influence and background conditions.

The air inlet heights are 25 m above ground at the Hangzhou site, 53 m at the Linan site, and 10 m at Damingshan site. Atmospheric CH_4 concentrations at all three sites were continuously measured using a cavity ring-down spectroscopy analyzer (model G2301 for Hangzhou site and G2401 for Linan site and Damingshan site; Picarro Inc., Sunnyvale, CA). To obtain high-precision observations, two different standard gases were measured and a linear two-point fit was used to calibrate the observations, and the precision of this instrument was within 2 ppb. Additional details of the observation and calibration systems are descripted in Fang et al., (2014; 2022). Note that because of instrument issues at the Damingshan site, a data gap occurred in September and October, 2021. In general, 99.4%, 99.0%, 79.3% of the hourly CH_4 observations were available for the entire observation period for the Hangzhou site, Linan site and Damingshan site, respectively. Meteorological observations at the Hangzhou meteorological station were used to evaluate simulated meteorological fields, including air temperature at 2 m (T_{2m}), relative humidity (RH), downward solar radiation (S↓), and wind speed (WS) at 10 m height.

Previous studies of city-scale greenhouse gas concentration observation networks have selected sites at the edge of urban borders as the background in the emission inversion system (i.e. Indianapolis, U.S.A., Miles et al., (2017); Los Angeles, U.S.A., Verhulst et al., (2017); Washington, DC-Baltimore, U.S.A., Lopez-Coto et al., (2020); Paris, France, Lian et al., (2021)); however, we used five CH_4 background sites as the potential background to be selected, including the UUM, TAP, YRO, YON and WLG site (Figure 1a), which were much further than the observations at the Damingshan site. This strategy is based on the following three reasons: (1) our footprint domain is much larger than Hangzhou city, and these five sites are also located close to the edge of model

https://doi.org/10.5194/acp-2022-549
Preprint. Discussion started: 17 October 2022


Atmospheric Chemistry and Physics Discussions

domain; (2) CH_4 concentrations within Hangzhou city will be influenced by seasonal varied monsoon, and the monthly varied wind directions will lead to obvious changes in the CH_4 background than only at the Damingshan site; and (3) our model setups can partition CH_4 enhancements within Hangzhou city and other regions.

The projected climate data from four Representative Concentration Pathway (RCP) scenarios (RCP8.5, RCP6.0, RCP4.5 and RCP2.6) using the MRI-CGCM3 model were downloaded from the World Data Center for Climate (WDCC, https://www.wdc-climate.de/ui/), where the annual air temperature at 2m was used from years 2021 to 2100. The most recent population density data for Hangzhou city were for the year of 2019, and they were downloaded from the Chinese National Resource and Environmental Science and Data Center (http://www.resdc.cn/DOI),2017. DOI:10.12078/2017121101).

2.2 WRF-STILT model setup

The Weather Research and Forecasting (WRF, version 4.2.2)-Stochastic Time-Inverted Lagrangian Transport (STILT) model will be used to simulate the hourly footprint and CH_4 enhancement (see more details in Hu et al., 2019, 2021). Domain setups are displayed in Figure 1a, with the outer nested domain (Domian-1, 27 km×27 km grid resolution) covering eastern and central China and the inner domain (Domain-2, 9 km×9 km grid resolution) covering the YRD area. The physical schemes used in the WRF model were the same as those used in our previous studies for the YRD domain (Hu et al., 2019; 2021). The simulated CH_4 concentration is the sum of background and enhancement, where the enhancement is calculated by multiplying all CH_4 flux by the hourly footprint that represents the sensitivity of the concentration changes to its regional sources/sinks with a spatial resolution of $0.1^o \times 0.1^o$. To better quantify the CH_4 components at each site, CH_4 enhancements from different regions and sources were also tracked and separately simulated. In addition, it should be noted that the CH_4 background is important in simulating CH_4 concentrations and atmospheric inversion. We selected the CH_4 background from the five background sites based on the monthly footprint, as discussed in Section 3.1.

The most recent EDGAR v6.0 inventory, which has 20 categories, was used for the anthropogenic

https://doi.org/10.5194/acp-2022-549
Preprint. Discussion started: 17 October 2022

Atmospheric Chemistry and Physics Discussions

237 CH_4 emissions. The main sources in Hangzhou city include solid waste landfills (SWD_LDF),
238 waste water handling (WWT), solid waste incineration (SWD_INC), fuel exploitation from coal,
239 oil, and natural gas (PRO), energy for buildings (RCO) and agricultural soils (AGS). We found
240 that emissions from SWD_LDF, WWT and SWD_INC were simply assigned to the same locations
241 in EDGAR inventory and hence were combined as waste treatment. For CH_4 emissions from
242 wetland, we used the WetCHARTs ensemble mean with a spatial resolution of 0.5° for the monthly
243 average (Bloom et al., 2017). Considering that the WetCHARTs treats rice paddies (the main
244 source of AGS) as one wetland type, the AGS in EDGAR was excluded, and we assumed that
245 WetCHARTs represent all wetland CH_4 emissions as natural wetlands and rice paddies.
246
247 2.3 **Bayesian inversion framework**
248 The Scale Factor Bayesian inversion (SFBI) approach was applied to interpret atmospheric CH_4
249 concentration (or enhancement) variations in terms of quantitative constraint on all CH_4 sources.
250 The relationship between the observed and simulated CH_4 concentrations (or enhancement) can be
251 expressed as follows in Equation 1:

252 $$y = \mathrm{K}\Gamma + \varepsilon \qquad (1)$$

253 where y is the observed CH_4 concentration (or enhancement), K corresponds to simulated
254 enhancements from all categories, Γ is the state vector to be optimized and consists of *posteriori*
255 SFs for the corresponding categories in K, and ε is the observing system error.
256
257 The optimal solution to derive *posteriori* SFs is to minimize the cost function J(Γ), which
258 represents the mismatch between CH_4 observations and simulations and the mismatch between
259 *posteriori* and *a priori* SFs (Miller et al., 2008; Griffis et al., 2017). The cost function J(Γ) can be
260 expressed as follows:

261 $$\mathrm{J}(\Gamma) = \frac{1}{2}\left[(y-\mathrm{K}\Gamma)^T S_e^{-1}(y-K\Gamma) + (\Gamma-\Gamma_a)^T S_a^{-1}(\Gamma-\Gamma_a)\right] \qquad (2)$$

262 where S_e and S_a are the constructed error covariance matrices for the observations and the *a*
263 *priori* values, respectively, and S_e consists of measurement and model errors. Here, each element
264 in the *a priori* SFs Γ_a is treated as 1. Therefore, the solution for obtaining the *posteriori* SFs is to
265 solve $\nabla_\Gamma J(\Gamma) = 0$, and it is given as follows:

https://doi.org/10.5194/acp-2022-549
Preprint. Discussion started: 17 October 2022

Atmospheric Chemistry and Physics Discussions

$$\Gamma_{post} = (K^T S_e^{-1} K + S_a^{-1})^{-1} (K^T S_e^{-1} y + S_a^{-1} \Gamma_a) \quad (3)$$

In the Bayesian inversion framework, we first need to estimate the error covariance matrices and state vector for the *a priori* and observational data. And following our previous studies conducted in East China (Hu et al., 2019; 2022). The uncertainty of 10%, 13% and 20% were assigned to the measurement errors (S_{obs}), finite number of particles (500) released in the STILT model ($S_{particles}$) and uncertainty in meteorological fields (S_{met}), respectively.

To provide robust constraints on CH_4 emissions, we used three cases of *a priori* uncertainty combinations for different emissions in Bayesian inversion as follows: (1) the first case uses three elements: wetland, waste treatment, and the rest anthropogenic sources, considering the larger seasonality of waste treatment, the uncertainties of 300% were used for waste treatment and 200% for other categories; (2) the second case has more detailed categories, such as wetland, waste treatment, fuel exploitation, energy for building, and the rest anthropogenic sources, where an *a priori* uncertainty of 200% was used for each category; and (3) the third case had the same categories as case 1 but used a different *a priori* uncertainty for waste treatment of 200%. The averages of all three cases are used as the final *posteriori* SFs, and the largest difference between each of the three cases is used as the uncertainty.

3. Results

3.1 Atmospheric CH_4 observations

We first displayed the hourly CH_4 concentrations from our three tower-based sites and smoothed the background at five sites using the CCGCRV fitting method, as shown in Figure 2a. The hourly observations at the three towers showed similar temporal variations but with different amplitude. Observations at the Hangzhou site displayed variations between 2000 ppb and 2800 ppb and were much larger than those at the Linan and Damingshan sites. Their monthly averages were also compared in Figure 2b, and results showed the monthly CH_4 varied between lowest 2106.3 ppb in July and highest 2225.0 ppb in September (annual mean of 2159.9 ppb) at the Hangzhou site, lowest 2023.3 ppb in July and highest 2132.0 ppb in September (annual mean of 2086.7 ppb) at the Linan site, the lowest 1955.5 ppb in July and without observations in September at the

https://doi.org/10.5194/acp-2022-549
Preprint. Discussion started: 17 October 2022


Atmospheric Chemistry and Physics Discussions

295 Damingshan site (annual mean of 2013.4 ppb). The similar variations among the three sites can be
296 explained by the fact that they were dominated by similar atmospheric transport processes;
297 however, their surrounding emission sources were highly different, implying that the emissions
298 from the Hangzhou site should be much larger than those from the Linan and Damingshan sites.
299
300 Because the CH_4 background is important in concentration simulation and emission inversion, we
301 also compared CH_4 background between the five sites, where the annual averages at TAP, YON,
302 RYO, WLG and UUM were 1989.8 ppb, 1850.1 ppb, 1982.7 ppb, 1973.4 ppb, and 1984.2 ppb,
303 respectively. We found that the differences were generally within 20 ppb among the TAP, RYO,
304 WLG and UUM sites (Figure 2), although a large difference was observed between the YON site
305 and the other four sites from May to August, and it reached approximately 100 ppb. Note that the
306 YON site was located to the south of the East China Sea (Figure 1a) and may be influenced by
307 monsoon with clean air flows from the South China Sea, which have much fewer CH_4 sources
308 than air flows from the Asian land area. The CH_4 background at the TAP site appeared slightly
309 higher than at the other four sites because the YON site is located on the coast of South Korea and
310 can be more easily polluted by anthropogenic emissions. Considering the large temporal
311 difference between CH_4 background sites, monthly air flows and source footprint were used to
312 identify backgrounds for our observation network, with details discussed in the Supplementary
313 Material (Section S2, Figure S3 and Table S1).
314
315 **3.2 Concentration footprint and *a priori* emissions**
316 To illustrate the potential source regions of the three sites, the annual averages of the simulated
317 footprints for each site are displayed in Figure 3a-c. The results show that their footprint
318 distributions were quite similar because of the close distance, although we also noticed that
319 obvious differences occurred in the footprint strength (i.e., the area covered by red color), with
320 Hangzhou site > Linan site > Damingshan site. The reason why the footprint at the Damingshan
321 site is the lowest is that observations were conducted at a height of 1500 m, which increased the
322 difficulty of receiving emission signals within boundary layer heights. In addition, the Hangzhou
323 site is located in the core urban area of Hangzhou city and will have a higher nighttime PBLH

https://doi.org/10.5194/acp-2022-549
Preprint. Discussion started: 17 October 2022


Atmospheric Chemistry and Physics Discussions

caused by anthropogenic heat and high buildings than the grassland/farmland-dominated Linan and Damingshan sites; hence, more air particles can be retained within the PBLH, which will generate a stronger footprint.

The *a priori* EDGAR CH_4 emissions for total anthropogenic categories, waste treatment and their proportions are further illustrated in Figure 3d-f, which reveals significant gradients from higher emissions in the east to lower emissions in the west, which is consistent with our three tower-based observations. The CH_4 emissions for waste treatment displayed similar spatial distributions to urban land use and population density (Figure 1c-d), and waste treatment seemed to emit CH_4 from area sources instead of point sources as waste treatment super plants. We should note that the Chinese government constructed waste separation stations in each city with a density of one station for per 150~200 households (around 450–800 people), and they can emit a large amount of methane from daily biomass waste as an area source. These above analyses also imply that the Hangzhou site can produce higher emissions from both waste treatment and total anthropogenic emissions, which will be discussed and quantified later.

3.3 Simulation of CH_4 concentrations and its components for three sites

Comparisons between the observed and simulated daily CH_4 concentration averages are displayed in Figure 4a-c and hourly concentrations are displayed in Figure S4 for the three sites. First, the hourly simulations in Figure S4 showed high consistence when only comparing the temporal patterns with observations, thus indicating the good performance of model transport simulations as confirmed in Figure S5, for evaluating meteorological fields. However, the amplitudes displayed obvious differences among the three sites for daily averages in Figure 4a-c. For the Hangzhou site, the simulated CH_4 concentrations showed obvious overestimation from October to April. The Damingshan site presented overestimated values, while the Linan site presented overestimated values from January to April and underestimated values from May to September. Considering that the source area contributions for the three sites are different, these differences among three sites indicated that the bias in CH_4 emission largely varied from the Hangzhou city scale to a larger regional scale.

https://doi.org/10.5194/acp-2022-549
Preprint. Discussion started: 17 October 2022


Atmospheric Chemistry and Physics Discussions

353 To further quantify the detailed contributions from different regions and categories to each tower
354 site, CH_4 enhancements from different categories and source areas were simulated separately for
355 the three sites. As displayed in Figure 4d-e, the simulated *a priori* total enhancements at the
356 Hangzhou, Linan, and Damingshan sites were 244.3 ppb, 100.8, and 69.0 ppb, respectively. We
357 also found that contributions by waste treatments dominated the total enhancements but with
358 obvious differences among the three sites, which varied from the highest 64.2% at the Hangzhou
359 site to the lowest of 41.4% at the Damingshan site. We further calculated anthropogenic
360 contributions from Hangzhou city (excluding wetland because of the coarser spatial resolution for
361 Hangzhou city) and other provinces, which were 158.4 ppb at the Hangzhou site, 30.7 ppb at the
362 Linan site, and 10.1 ppb at the Damingshan site, respectively. These accounted for 69.3%, 34.0%,
363 and 16.9% of the total anthropogenic enhancements at the corresponding sites. These results
364 indicated that the CH_4 observations at the Hangzhou site, which is located in the core urban region,
365 were more influenced by local emissions and contained much higher enhancements than the other
366 two sites; moreover, they show that the observations at the Linan and Damingshan sites can
367 present CH_4 emissions of much larger regions, such as Zhejiang province or YRD, than Hangzhou
368 city (Figure 4e).
369
370 The seasonal-averaged diurnal variations for both the observations and simulations are also
371 displayed in Figure 5 for the three sites. Although many previous studies only used daytime
372 observations and simulations to evaluate *a priori* emissions bias and constrain emissions (Sargent
373 et al., 2018; Hu et al., 2022), these studies were based on the assumption that the diurnal scaling
374 factors used on *a priori* emissions are correct (i.e., for anthropogenic CO_2) or the emissions do not
375 have obvious diurnal variations (i.e., emissions from industries or manufacturing). As concluded
376 above, the main CH_4 component in Hangzhou city was waste treatment (Figure 3f), which should
377 be highly sensitive to temperature and have obvious diurnal patterns, with larger emissions during
378 the daytime and smaller emissions at nighttime. Its emissions will be overestimated if only
379 daytime observations and emissions were used to represent daily averages. Furthermore, we found
380 high similarities in the diurnal variations between observations and simulations for the three sites,
381 although some discrepancies were observed. For example, the observations at the Linan site were

https://doi.org/10.5194/acp-2022-549
Preprint. Discussion started: 17 October 2022


Atmospheric Chemistry and Physics Discussions

382 generally higher than the simulations from spring to autumn for both all-day and midday averages.
383
384 Hence, our preliminary conclusions were that the *a priori* CH_4 emissions were generally
385 overestimated for Hangzhou city but underestimated in larger regions, such as Zhejiang and YRD
386 areas. We also found that simulations were higher than observations for all seasons at the
387 Damingshan site, which can be explained by the high heterogeneity around the Damingshan site,
388 where elevations changed from 0 m to 1600 m within the site located in the grid cell of 9 km (~
389 0.1°), as displayed in Figure 1b. Moreover, the mountain-valley wind and PBLH changes can only
390 be resolved with much higher spatial resolutions as < 1km. Hence, the use of coarse resolutions
391 (i.e. 9 km in this study) in the mountainous regions will bring a large bias in simulating
392 concentration and emission inversion, as was recently found in China for CO_2 as "aggregation
393 error" (Agustí-Panareda et al., 2019; Wang et al., 2022); therefore, observations at the
394 Damingshan site will not be used in emission inversions in this study.
395
396 **3.4 Constraint on anthropogenic CH_4 emissions**
397 As shown in Figures 3f and 5a and Section 3.3, simulations using *a priori* CH_4 emissions showed
398 obvious overestimations, especially from October to April at the Hangzhou site, and
399 overestimations in winter and underestimations from spring to autumn at the Linan site,
400 respectively. This bias can be attributed to *a priori* emissions or meteorological simulations. Our
401 previous studies in the YRD have evaluated the meteorological simulations using the same
402 physical parameterization schemes, which showed high consistence with the observations (Hu et
403 al., 2019; 2021; 2022; Huang et al., 2021). We also evaluated meteorological simulations with
404 observations and confirmed their good model performance (Figure S5). Furthermore, we found no
405 monthly variations in EDGAR v6.0 CH_4 emissions occurred for waste treatment, which
406 contributed 64.2% to the annual CH_4 enhancement average and was much higher in winter (Figure
407 S6). CH_4 emissions from waste treatment are contributed by a microbial process that should be
408 affected by meteorological conditions, especially seasonal temperature changes. Hence, our
409 assumption was that bias in both its seasonality and annual average led to large
410 overestimation/underestimation in the simulated CH_4 concentration. In addition, the bias in other

https://doi.org/10.5194/acp-2022-549
Preprint. Discussion started: 17 October 2022


Atmospheric Chemistry and Physics Discussions

411 anthropogenic emissions and wetlands can also partly contribute to the bias of the simulated CH_4
412 concentration.
413
414 To quantify the bias sources and constrain the corresponding *a priori* emissions for Hangzhou city,
415 we applied the scaling factor Bayesian inversion approach with three different cases, as introduced
416 in the Methods section. Instead of using only daytime CH_4 observations to constrain *a priori*
417 emissions, we chose to use all-day hourly data at the Hangzhou site to constrain emissions for
418 Hangzhou city, which is based on the following three reasons. (1) The enhancement contributed
419 by Hangzhou city at the Hangzhou site was 69.3%, which was much larger than 34.0% and 16.9%
420 for the Linan and Damingshan sites, respectively. (2) Waste treatment dominated anthropogenic
421 CH_4 emissions in Hangzhou city because of biological processes and should be
422 temperature-dependent. The observed temperature displays obvious diurnal variations at 20 ^oC,
423 and the use of only daytime observations without considering diurnal CH_4 emissions will
424 introduce significant bias when using derived daytime emissions to represent all-day averages. (3)
425 Previous studies using daytime observations were mainly conducted in regions dominated by
426 industry or energy production, and these contributors have much smaller diurnal variations than
427 waste treatment.
428
429 The derived monthly *posteriori* SFs for each emission source for Hangzhou city are displayed in
430 Table 1. The results showed that the *posteriori* SFs for waste treatment were much smaller in
431 winter and higher in summer, indicating obvious seasonality. The overestimation in winter was
432 mainly contributed by waste treatment. The annual mean *posteriori* SFs for waste treatment varied
433 between 0.50 and 0.56 in all three cases, indicating overestimations in the annual average for the *a*
434 *priori* waste treatment emissions. In addition, the annual mean *posteriori* SFs varied between 0.87
435 and 0.94 for the remaining anthropogenic categories (excluding agricultural soil) and between
436 1.05 and 1.05 for wetlands (including agricultural soil and natural wetland); thus, only slight bias
437 was observed for other anthropogenic categories and wetlands.
438
439 To evaluate whether the *posteriori* SFs significantly improved CH_4 emissions, we used these SFs

https://doi.org/10.5194/acp-2022-549
Preprint. Discussion started: 17 October 2022


Atmospheric Chemistry and Physics Discussions

to derive the *posteriori* emissions and re-simulated hourly concentrations shown in Figure 6 (and daily averages in Figure S7). The results showed that the hourly overestimation produced using *a priori* emissions was largely reduced by using *posteriori* emissions when compared with the observations shown in Figure 6a-b, and the regression slope between daily averaged observations and simulations decreased from 1.51(±0.15) for the *a priori* simulations to 0.85(±0.07) for the *posteriori* simulations in Figure 6c. The mean bias (MB), root mean squared error (RMSE), and correlation coefficient (R) between daily observations and *a priori* simulations were 64.1 ppb, 129.2 ppb and 0.44, respectively, and these statistics changed to -22.2 ppb, 72.3 ppb and 0.58 for *posteriori* simulations. These results indicate that the *posteriori* SFs obviously decreased the bias in the *a priori* emissions and were close to the observations.

Comparisons of the monthly CH_4 emissions between the *a priori* and *posteriori* waste treatment and other anthropogenic sources (excluding agricultural soil) in Hangzhou city are displayed in Figure 7a. For the *a priori* inventory, seasonal variations were not observed for waste treatment with constant monthly emissions of 8.67×10^3 t, and other anthropogenic sources showed seasonality that was much higher in winter (i.e., 5.22×10^3 t in January) than in summer (i.e., 3.06×10^3 t in August). As discussed above, the constant emissions from waste treatment should be incorrect because of its large temperature sensitivity, and the observed monthly temperature difference between summer and winter was larger than 25°C in Hangzhou city. After applying the constraint by using the observed concentration, the *posteriori* emissions for waste treatment showed obvious seasonality, with the highest value in July ($7.66 \pm 0.09 \times 10^3$ t) and lowest in February ($2.20 \pm 0.87 \times 10^3$ t). In addition, the other anthropogenic emissions showed much smaller seasonality (highest in January of $4.18 \pm 0.69 \times 10^3$ t and lowest in August of $2.88 \pm 0.15 \times 10^3$ t) than the *a priori* emissions. In general, the annual emission from waste treatment was 10.4×10^4 t in the *a priori* EDGAR inventory and decreased by 47.1% to 5.5 $(\pm 0.6) \times 10^4$ t for the *posteriori* emissions. The *a priori* emissions from other anthropogenic sources was 4.5×10^4 t and only slightly decreased by 8.9% to 4.1 $(\pm 0.3) \times 10^4$ t for the *posteriori* emissions. The proportion of waste treatment to the total anthropogenic emissions decreased from 69.3% to 57.3%. To sum it up, the annual total anthropogenic CH_4 emissions (excluding agricultural soil) decreased from

https://doi.org/10.5194/acp-2022-549
Preprint. Discussion started: 17 October 2022


Atmospheric Chemistry and Physics Discussions

469 15.0×10^4 t to 9.6 (±0.9)$\times10^4$ t, indicating an overestimation of 36.0% in Hangzhou city for the *a*
470 *priori* emissions.
471
472 However, as indicated above, the observations and simulations at the Linan site, which represents
473 a much larger region, such as Zhejiang Province or YRD area, illustrated different results in that
474 CH_4 simulations were underestimated from spring to autumn and overestimated in winter (Figure
475 4b and Figure 5e-h). Here, we used the multiplicative scaling factor (MSF) method and
476 observations at the Linan site to derive SFs on a seasonal scale (Sargent et al., 2018; He et al.,
477 2020), and 10 ppb was used as the potential CH_4 background uncertainty in winter, spring, and
478 autumn while 20 ppb was used in summer (see details in the Supplementary Material (Section
479 S2)). The derived *posteriori* SFs were 0.87 (±0.08), 1.07 (±0.11), 1.19 (±0.24), and 1.16 (±0.11)
480 for winter, spring, summer, and autumn, respectively. Similar seasonal variations as those found
481 for Hangzhou city were observed, and they were 1.07 (±0.14) of the *a priori* anthropogenic
482 emissions for the annual average. Our observations at the Hangzhou and Linan sites together
483 indicate that the *a priori* emissions are largely biased at both seasonal and annual scales, and the
484 annual anthropogenic CH_4 emissions were largely overestimated by 36.0% in Hangzhou city but
485 underestimated by 7.0% in the larger region of the Zhejiang Province or YRD area.
486
487 **3.5 Temperature sensitivity of the waste treatment CH_4 EFs and projected changes**
488 Although the derived *posteriori* monthly SFs for waste treatment reflected changes in emissions,
489 considering that the monthly activity data do not present obvious monthly changes, these SFs can
490 mainly reflect relative variations of monthly EFs and contain meteorological changes, especially
491 temperature. To evaluate the temperature sensitivity of the EFs, we first calculated the normalized
492 monthly SFs by dividing the monthly SFs by the annual averages (Table S2) and quantified the
493 relationship between the observed T_{2m} and normalized SFs. The normalized SFs illustrated a
494 significant linear relationship with monthly T_{2m} (Figure 7b), where the slopes imply that
495 normalized SFs (and EFs) will increase by 38–50% with a temperature increase of 10ºC at the city
496 scale.
497

https://doi.org/10.5194/acp-2022-549
Preprint. Discussion started: 17 October 2022


Atmospheric Chemistry and Physics Discussions

Our findings on the high sensitivity of waste treatment CH_4 emissions to temperature also indicated a dramatic increase based on the projected future global warming trends. We further derived the T_{2m} trends for four different RCP scenarios RCP8.0, RCP6.0, RCP4.5 and RCP2.6 (Figure 8a), and the results showed that T_{2m} will increase by 0.50, 0.28, 0.16ºC, and 0.10ºC per decade for Hangzhou city, respectively. These different warming trends also indicate distinct temperature-dominated influences on future CH_4 EFs and emissions from waste treatment. We then used the slopes in Figure 7b and the annual temperature from 2021 to 2100 to derive relative changes in EF in the future 80 years, where the observation year of 2021 was treated as the baseline year. As displayed in Figure 8b, the EFs in RCP8.5, RCP6.0, RCP4.5, and RCP2.6 will increase by 2.2%, 1.2%, 0.7%, and 0.5% per decade, respectively, and the CH_4 EFs for waste treatment will increase by 17.6%, 9.6%, 5.6%, and 4.0% at the end of this century, respectively.

The spatial distribution of T_{2m} trends for the whole of China is also displayed in Figure S8, which shows heterogeneous distributions across China for the four global warming scenarios. Because East China has high population density and the majority of the national population (Figure S1), and owns the largest domestic garbage-induced CH_4 emissions (Figure S2), these combined factors indicate considerable CH_4 emission changes from waste treatment in such a temperature-sensitive area. If we assume that the derived temperature sensitivity (which increased by 44% with temperature increases of 10ºC on average) is applicable for all of China, especially for East China, the relative changes in waste treatment CH_4 EFs can be calculated by multiplying this value by the air temperature trends. The spatial distributions of global warming-induced EFs changes at the end of this century are displayed in Figure 9. For the RCP2.6 scenario, the EFs for waste treatment will slightly increase by 4.0-6.5% in the north of East China and increase by 3.0-4.0% in south of East China. The RCP6.0 scenario also displayed heterogeneous changes in East China, with the north of East China increasing by 10.5-13.0% and south of East China increasing by 9.0-10.5%. Relative changes in RCP4.5 and RCP8.5 are more homogeneous for East China, which indicates that EFs will significantly increase by 5.0-7.5% and 17.5-19.5%, respectively. The largest changes of >20.0% will occur in West China for RCP8.5, although this area has a low population density and CH_4 emissions, indicating negligible effects of global

https://doi.org/10.5194/acp-2022-549
Preprint. Discussion started: 17 October 2022


Atmospheric Chemistry and Physics Discussions

527 warming (Figure S8). Finally, we should note that these derived relative changes are only caused
528 by global warming and the influence of activity data, management technology, and other factors is
529 beyond the scope of this study.
530
531 **4 Discussions and implications**
532 Many previous studies have compared total CH_4 emissions and their components for different
533 inventories and bottom-up methods, which illustrated large uncertainty and bias at the city scale,
534 and these biases are much larger for waste treatment (Peng at al., 2016; Saunois et al., 2020; Lin et
535 al., 2021; Bian et al., 2022). A recent bottom-up study compared wastewater CH_4 EFs in China,
536 which largely varied by four-fold in different provinces and the uncertainty in the same province
537 was even two-fold larger than its average, implying considerable bias in recent understanding of
538 waste treatment EFs at the regional scale (Hua et al., 2022). The total national emissions varied
539 between 5 and 15 Tg a^{-1} (Peng et al., 2016; EDGAR v6). Other atmospheric inversion studies
540 have estimated China's CH_4 emissions (Hopkins et al., 2016; Hu et al., 2019; Huang et al., 2021;
541 Miller et al., 2019; Lu el., 2021; Chen et al., 2022) and found a large bias in nation-wide emissions
542 for almost all inventories, which was mainly caused by fossil fuel exploitation, the agricultural
543 sector (livestock and rice paddies), and waste treatment. For comparisons of waste treatment
544 emissions, these satellite-based inversions also varied between 6 and 9 Tg a^{-1} by 1.5-fold (Miller
545 et al., 2019; Lu et al., 2021; Chen et al., 2022).
546
547 The above discrepancies between "bottom-up" and "top-down" approaches indicate large
548 uncertainty in understanding China's national CH_4 emissions from waste treatment. Uncertainties
549 increase from the national to regional and city scales, and considerable bias is observed in
550 city-scale emissions for inventories. However, few studies in China and worldwide have
551 performed atmospheric inversions for city-scale waste treatment especially by using tower-based
552 observations, which can present an independent evaluation method. To the best of our knowledge,
553 only one recent research study performed an atmospheric inversion that focused on waste
554 treatment, and it used satellite-based observations to constrain emissions from four cities in India
555 and Pakistan and concluded that total CH_4 emissions were underestimated by 1.4 to 2.6 times for

https://doi.org/10.5194/acp-2022-549
Preprint. Discussion started: 17 October 2022


Atmospheric Chemistry and Physics Discussions

the EDGAR inventory, where emissions from landfills accounted for 6~50% of total emissions (Maasakkers et al., 2022). In our study, we found that the annual waste CH_4 emissions were overestimated by 47.1% for Hangzhou city, which is different from the results in India and Pakistan. These differences indicate that the bias in waste treatment CH_4 emissions vary considerably in different countries and based on climate divisions. Our results highlight a large knowledge gap in terms of emission mechanisms and urban waste treatment CH_4 emissions estimates, especially in China.

Compared with other fossil-type sources that have much smaller monthly variations, waste treatment is microbial process-based and its EFs are highly sensitive to meteorological conditions, especially temperature. These factors lead to an obvious bias in waste treatment CH_4 emissions in terms of the annual average and its seasonality. Although a few studies have predicted future CH_4 emissions from waste treatment, these studies were mainly based on activity data changes and did not consider EF variations caused by future global warming trends, or were only based on site-specific observations (USEPA 2013; Cai et al., 2018; Spokas et al., 2021). To the best of our knowledge, no inventories have considered temperature-induced changes in its seasonal variations and annual trends. Hence, how EFs change under different global warming scenarios at the city scale has not been clarified.

A few observation-based measurements have been conducted for waste treatment but only at specific sites with large discrepancies in EFs (Du et al., 2017; 2018; Cai et al., 2018; Zhao et al., 2019; NBSC, 2015; Wang et al., 2015; Florentino et al., 2010; Tolaymat et al., 2010; Cai et al., 2014; 2018). Only one previous study used year-round atmospheric CH_4 observations to constrain regional scale CH_4 emissions in Nanjing city in the YRD area (Huang et al., 2021), and it revealed much higher emissions of landfilling waste in summer than in winter, with the emissions in July approximately four times higher in February. However, previous studies have not quantified the temperature sensitivity of waste CH_4 emissions at the city scale or at much larger regional scales. These two studies in different cities confirmed that temperature was the dominant factors driving seasonal variations in waste treatment CH_4 emissions. Hence, our study is the first to estimate

https://doi.org/10.5194/acp-2022-549
Preprint. Discussion started: 17 October 2022


Atmospheric Chemistry and Physics Discussions

585 city-scale waste treatment CH_4 emissions, their temperature sensitivity, and projected changes in
586 different global warming scenarios. Our findings regarding the large sensitivity of temperature
587 indicate that monthly scaling factors should be considered to better simulate atmospheric CH_4
588 concentrations.
589
590 We also note that the predictions of future climate change were mainly based on different emission
591 intensities of greenhouse gases and CH_4 contributed approximately 20% of direct anthropogenic
592 radiative forcing (Seto et al., 2014). The CH_4 emissions in different global warming scenarios
593 were mainly calculated by predicting the energy use data without considering the changes in the
594 EFs. In this study, we found that there should be a large positive feedback between global
595 warming and CH_4 emissions, especially in the RCP8.0 scenario, where global warming induced
596 emissions will increase by 17.6%. Hence, projected emissions from waste treatments and other
597 biological process-based sources together with positive feedback between temperature and their
598 emissions should be included in future climate change models. In addition, CH_4 concentration
599 simulations are essential for modeling many air pollutants (i.e., O_3, NO_x, and CO), especially in
600 the stratosphere (Isaksen et al., 2011; Kaiho et al., 2013). Considering that waste treatment CH_4
601 emissions accounted for ~25% of total anthropogenic emissions (EDGAR v6.0) in East China,
602 where severe air pollution frequently occurs, we also believe that the coupling of
603 temperature-dependent CH_4 emissions and the monthly scaling factors for CH_4 emissions can
604 improve air pollution modeling in East China.
605
606 **5 Conclusions**
607 CH_4 emissions from waste treatment ranks as one of the main global anthropogenic sources,
608 although estimations of its emissions at the city scale still have large biases and uncertainties,
609 especially in the megacities of developing countries. To better evaluate bias for city-scale
610 anthropogenic CH_4 emissions and understand the sensitivity of temperature to waste treatment
611 CH_4 emissions, we conducted three tower-based atmospheric CH_4 observation networks in
612 Hangzhou city, which is located in the developed YRD region and one of the top 10 megacities in
613 China. One-year hourly atmospheric CH_4 observations were presented from December 2020 to

https://doi.org/10.5194/acp-2022-549
Preprint. Discussion started: 17 October 2022


Atmospheric Chemistry and Physics Discussions

November 2021. We then applied a scaling factor Bayesian inversion method to constrain the monthly anthropogenic CH_4 emissions and components (especially for waste treatments) in Hangzhou city, and used the multiplicative scaling factor method for the broader Zhejiang Province and YRD area on a seasonal scale.

To the best of our knowledge, this study produced the first tower-based CH_4 observation network in China. We found an obvious seasonal bias of simulated CH_4 concentrations in the core urban area of Hangzhou city, and it was mainly caused by bias of waste treatment at both annual and monthly scales. The derived *posteriori* CH_4 emissions displayed significant seasonal variations, with a peak in summer and trough in winter that were mainly caused by waste treatment. The *a priori* annual waste treatment CH_4 emission in Hangzhou city was 10.4×10^4 t, while the *posteriori* emissions decreased by 47.1% to 5.5 $(\pm0.6)\times10^4$ t. In addition, the total anthropogenic CH_4 emissions (excluding agricultural soil) decreased from 15.0×10^4 t to $9.6(\pm0.9)\times10^4$ t, thus indicating an overestimation of 36.0% for the whole year of 2021. Observations at the Linan site imply that the annual CH_4 emissions were slightly underestimated by 7.0% in a larger region of Zhejiang Province or the YRD area, which was different from the observations at Hangzhou city. Additionally, the *posteriori* monthly CH_4 emissions from waste treatment illustrated a significant linear relationship with air temperature, with the regression slopes indicating an increase of 38–50% when the temperature increased by 10°C. Finally, we found that the waste treatment CH_4 EFs for Hangzhou city increased by 17.6%, 9.6%, 5.6%, and 4.0% at the end of this century for RCP8.0, RCP6.0, RCP4.5, and RCP2.6, respectively. The derived relative changes for all of China also showed high heterogeneity and indicated large uncertainty in projecting future national total CH_4 emissions. This study is the first to focus on the city-scale temperature sensitivity of waste treatment CH_4 emissions from the perspective of the atmospheric inversion approach. Based on the above results, we strongly suggest that temperature-dependent EFs should be coupled within both recent CH_4 inventories and future CH_4 emission projections.

Data availability: The atmospheric CH_4 observations data can be requested from Cheng Hu and Bing Qi. STILT model is downloaded from http://www.stilt-model.org/, the EDGAR inventory is from https://edgar.jrc.ec.europa.eu/, and the projected climate data were downloaded from World

https://doi.org/10.5194/acp-2022-549
Preprint. Discussion started: 17 October 2022

Atmospheric Chemistry and Physics Discussions

Data Center for Climate (WDCC, https://www.wdc-climate.de/ui/).

Acknowledgement: Cheng Hu is supported by the National Natural Science foundation of China (grant no. 42105117) and Natural Science Foundation of Jiangsu Province (grant no. BK20200802). Wei Xiao is supported by the National Key R&D Program of China (grants 2020YFA0607501 & 2019YFA0607202). This work is also supported by Zhejiang Provincial Basic Public Welfare Research Project (LGF22D050004).

Author contribution: Cheng Hu and Bing Qi designed the study. Cheng Hu performed the model simulation, data analysis and wrote the paper; Bing Qi and Rongguang Du conducted CH_4 concentration observation and meteorological data collection, and all co-authors contributed to the data/figures preparation and analysis.

Declaration of competing interests: The authors declare that they have no conflict of interest.

References:

Agustí-Panareda, A., Diamantakis, M., Massart, S., Chevallier, F., Muñoz-Sabater, J., Barré, J., Curcoll, R., Engelen, R., Langerock, B., Law, R. M., Loh, Z., Morguí, J. A., Parrington, M., Peuch, V.-H., Ramonet, M., Roehl, C., Vermeulen, A. T., Warneke, T., and Wunch, D.: Modelling CO_2 weather – why horizontal resolution matters, Atmos. Chem. Phys., 19, 7347–7376, https://doi.org/10.5194/acp-19-7347-2019, 2019.

Bian R., Zhang T., Zhao F., et al. Greenhouse gas emissions from waste sectors in China during 2006–2019: Implications for carbon mitigation. Process. Saf. Environ., 161:488-497, 2022.

Bloom, A. A., Bowman, K. W., Lee, M., Turner, A. J., Schroeder, R., Worden, J. R., Weidner, R., McDonald, K. C., and Jacob, D. J.: A global wetland methane emissions and uncertainty dataset for atmospheric chemical transport models (WetCHARTs version 1.0), Geosci. Model Dev., 10, 2141–2156, https://doi.org/10.5194/gmd-10-2141-2017, 2017.

Cai, B., J. Liu, X. Zeng, D. Cao, L. Liu, Y. Zhou, Z. Zhang, Estimation of CH_4 emission from landfill in China based on point emission sources. Adv. Clim. Change Res. 5, 81–91, 2014.

Cai, B., Lou, Z., Wang, J., Geng, Y., Sarkis, J., Liu, J., and Gao, Q.: CH_4 mitigation potentials from China landfills and related environmental co-benefits, Sci. Adv., 4, eaar8400, https://doi.org/10.1126/sciadv.aar8400, 2018.

Chen, Z., Jacob, D. J., Nesser, H., Sulprizio, M. P., Lorente, A., Varon, D. J., Lu, X., Shen, L., Qu, Z., Penn, E., and Yu, X.: Methane emissions from China: a high-resolution inversion of TROPOMI satellite observations, Atmos. Chem. Phys., 22, 10809–10826, https://doi.org/10.5194/acp-22-10809-2022, 2022.

Du, M., Peng, C., Wang, X., Chen, H., Wang, M., and Zhu, Q.: Quantification of methane emissions from municipal solid waste landfills in China during the past decade, Renew. Sust. Energ. Rev., 78, 272–279, 2017.

Du, M., Zhu, Q., Wang, X., Li, P., Yang, B., Chen, H., Wang, M., Zhou, X., and Peng, C.: Estimates and predictions of methane emissions from wastewater in China from 2000 to 2020, Earths Future, 6, 252–263, 2018.

https://doi.org/10.5194/acp-2022-549
Preprint. Discussion started: 17 October 2022

Atmospheric Chemistry and Physics Discussions

Fang S.X., R.G. Du, B. Qi. et al., Variation of carbon dioxide mole fraction at a typical urban area in the Yangtze River Delta, China. Atmos. Res, 265, 105884, 2022.

Florentino, Cruz., B. De La., and M. A. Barlaz., Estimation of waste component-specific landfill decay rates using laboratory-scale decomposition data. Environ. Sci. Technol. 44, 4722–4728, 2010.

Griffis, T. J., Chen, Z., Baker, J. M., Wood, J. D., Millet, D. B., Lee, X., et al., Nitrous oxide emissions are enhanced in a warmer and wetter world. P. Natl. Acad. Sci. USA, 114(45), 12081–12085. https://doi.org/10.1073/pnas.1704552114, 2017.

He, J., Naik, V., Horowitz, L. W., Dlugokencky, E., and Thoning, K.: Investigation of the global methane budget over 1980–2017 using GFDL-AM4.1, Atmos. Chem. Phys., 2020, 20, 805–827, https://doi.org/10.5194/acp-20-805-2020.

Henne, S., Brunner, D., Oney, B., Leuenberger, M., Eugster, W., Bamberger, I., Meinhardt, F., Steinbacher, M., and Emmenegger, L.: Validation of the Swiss methane emission inventory by atmospheric observations and inverse modelling, Atmos. Chem. Phys., 16, 3683–3710, https://doi.org/10.5194/acp-16- 3683-2016, 2016.

Hopkins, F. M., Kort, E. A., Bush, S. E., Ehleringer, J. R., Lai, C.-T., Blake, D. R., & Randerson, J. T. Spatial patterns and source attribution of urban methane in the Los Angeles Basin. J. Geophys. Res-Atmos., 121, 2490–2507, 2016.

Höglund-Isaksson, L.: Global anthropogenic methane emissions 2005–2030: technical mitigation potentials and costs, Atmos. Chem. Phys., 12, 9079–9096, https://doi.org/10.5194/acp-12- 9079-2012, 2012.

Hua, H., Jiang, S., Yuan, Z., Liu, X., Zhang, Y., & Cai, Z. Advancing greenhouse gas emission factors for municipal wastewater treatment plants in China. Environ. Pollut., 295, 118648. https://doi.org/10.1016/j.envpol.2021.118648, 2022.

Hu C, Griffis, T. J., Liu, S., Xiao, W., Hu, N., Huang, W., Yang, D., Lee, X., Anthropogenic methane emission and its partitioning for the Yangtze River Delta region of China. J. Geophys.l Res-Biogeo., 124(5): 1148-1170, 2019.

Hu, C., Xu, J., Liu, C., Chen, Y., Yang, D., Huang, W., Deng, L., Liu, S., Griffis, T. J., and Lee, X.: Anthropogenic and natural controls on atmospheric δ13C-CO2 variations in the Yangtze River delta: insights from a carbon isotope modeling framework, Atmos. Chem. Phys., 21, 10015–10037, https://doi.org/10.5194/acp-21-10015-2021, 2021.

Hu, C., Griffis, T.J., Xia, L., Xiao, W., Liu, C., Xiao, Q., Huang, X., Yang, Y., Zhang, L., Hou, B., Anthropogenic CO_2 emission reduction during the COVID-19 pandemic in Nanchang City, China, Environ. Pollut., 309, 119767, doi: https://doi.org/10.1016/j.envpol.2022.119767, 2022.

Huang, W. J., T. J. Griffis, C. Hu, W. Xiao, and X. H. Lee. Seasonal variations of CH_4 emissions in the Yangtze River Delta region of China are driven by agricultural activities. Adv. Atmos. Sci., 38(9), 1537−1551, https://doi.org/10.1007/s00376-021-0383-9, 2021.

https://doi.org/10.5194/acp-2022-549
Preprint. Discussion started: 17 October 2022

Atmospheric Chemistry and Physics Discussions

Isaksen I S, Gauss M, Myhre G, Anthony W, Katey M and Ruppel C 2011 Strong atmospheric chemistry feedback to climate warming from Arctic methane emissions. Global Biogeochem. Cy. 25 GB2002, 2011.

Lian, J., Bréon, F.-M., Broquet, G., Lauvaux, T., Zheng, B., Ramonet, M., Xueref-Remy, I., Kotthaus, S., Haeffelin, M., and Ciais, P.: Sensitivity to the sources of uncertainties in the modeling of atmospheric CO_2 concentration within and in the vicinity of Paris, Atmos. Chem. Phys., 21, 10707–10726, https://doi.org/10.5194/acp-21-10707-2021, 2021.

Lin, X., Zhang, W., Crippa, M., Peng, S., Han, P., Zeng, N., Yu, L., and Wang, G.: A comparative study of anthropogenic CH_4 emissions over China based on the ensembles of bottom-up inventories, Earth Syst. Sci. Data, 13, 1073–1088, https://doi.org/10.5194/essd-13-1073-2021, 2021.

Lopez-Coto, I., Ren, X., Salmon, O. E., Karion, A., Shepson, P. B., Dickerson, R. R., Stein, A., Prasad, K., and Whetstone, J. R.: Wintertime CO_2, CH_4, and CO Emissions Estimation for the Washington, DC-Baltimore Metropolitan Area Using an Inverse Modeling Technique, Environmental Science and Technology, 54, 2606–2614, https://doi.org/10.1021/acs.est.9b06619, 2020.

Lou, Z., Cai, B.F., Zhu, N., Zhao, Y., Geng, Y., Yu, B., Chen, W., Greenhouse gas emission inventories from waste sector in China during 1949–2013 and its miti- gation potential. J. Clean. Prod. 157, 118–124. https://doi.org/10.1016/j.jclepro. 2017.04.135, 2017.

Lu, X., Jacob, D. J., Zhang, Y., Maasakkers, J. D., Sulprizio, M. P., Shen, L., Qu, Z., Scarpelli, T. R., Nesser, H., Yantosca, R. M., Sheng, J., Andrews, A., Parker, R. J., Boesch, H., Bloom, A. A., and Ma, S.: Global methane budget and trend, 2010–2017: com- plementarity of inverse analyses using in situ (GLOBALVIEW- plus CH4 ObsPack) and satellite (GOSAT) observations, At- mos. Chem. Phys., 21, 4637–4657, https://doi.org/10.5194/acp-21-4637-2021, 2021.

Kaiho K., Koga S. Impacts of a massive release of methane and hydrogen sulfide on oxygen and ozone during the late Permian mass extinction. Global Planetary Change, 107:91-101, https://doi.org/10.1016/j.gloplacha.2013.04.004, 2013.

Maasakkers, J. D., Varon, D. J., Elfarsdóttir, A., McKeever, J., Jervis, D., Mahapatra, G., Pandey, S., Lorente, A., Borsdorff, T., Foorthuis, L. R., Schuit, B. J., Tol, P., van Kempen, T. A., van Hees, R., & Aben, I. Using satellites to uncover large methane emissions from landfills. Sci. Adv. 8, eabn9683, 10. https://doi.org/10.1126/sciadv.abn9683, 2022.

Masuda, S., Sano, I., Hojo, T., Li, Y., Nishimura, O., The comparison of greenhouse gas emissions in sewage treatment plants with different treatment processes. Chemosphere 193, 581–590, 2018.

Miles, N. L., Richardson, S. J., Lauvaux, T., Davis, K. J., Balashov, N. V., Deng, A., Turnbull, J. C., Sweeney, C., Gurney, K. R., Patarasuk, R., Razlivanov, I., Cambaliza, M. O. L. and Shepson, P. B.: Quantification of urban atmospheric boundary layer greenhouse gas dry mole fraction enhancements in the dormant season: Results from the Indianapolis Flux Experiment (INFLUX), Elem Sci Anth, 5, 27, doi:10.1525/elementa.127, 2017.

https://doi.org/10.5194/acp-2022-549
Preprint. Discussion started: 17 October 2022

Atmospheric Chemistry and Physics Discussions

Miller, S. M., Matross, D. M., Andrews, A. E., Millet, D. B., Longo, M., Gottlieb, E. W., Hirsch, A. I., Gerbig, C., Lin, J. C., Daube, B. C., Hudman, R. C., Dias, P. L. S., Chow, V. Y., and Wofsy, S. C.: Sources of carbon monoxide and formaldehyde in North America determined from high-resolution atmospheric data, Atmos. Chem. Phys., 8, 7673–7696, https://doi.org/10.5194/acp-8-7673-2008, 2008.

Miller, S. M., Michalak, A. M., Detmers, R. G., Hasekamp, O. P., Bruhwiler, L. M. P., & Schwietzke, S. China's coal mine methane regulations have not curbed growing emissions. Nature Communications, 10(1), 303–308. https://doi.org/10.1038/s41467-018-07891-7, 2019.

National Bureau of Statistics of China (NBSC), China Statistical Yearbook (China Statistics Press, 2015) (in Chinese).

Peng, S., Piao, S., Bousquet, P., Ciais, P., Li, B., Lin, X., Tao, S., Wang, Z., Zhang, Y., and Zhou, F.: Inventory of anthropogenic methane emissions in mainland China from 1980 to 2010, Atmos. Chem. Phys., 16, 14545–14562, https://doi.org/10.5194/acp-16-14545-2016, 2016.

Sargent, M., Barrera, Y., Nehrkorn, T., Hutyra, L. R., Gately, C. K., Mckain, K., Sweeney, C., Hegarty, J., Hardiman, B., Steven C. Wofsy, S. C.: Anthropogenic and biogenic CO_2 fluxes in the Boston urban region, P. Natl. Acad. Sci. USA., 115(40), https://doi.org/10.1073/pnas.1803715115, 2018.

Saunois, M., Stavert, A. R., Poulter, B., et al., The Global Methane Budget 2000–2017, Earth Syst. Sci. Data, 12, 1561– 1623, https://doi.org/10.5194/essd-12-1561-2020, 2020.

Seto, K. C. hakal, S. Bigio, A. Blanco, H. elgado, G. C. ewar,. Huang, L. Inaba, A. Kansal, A. Lwasa, S. cahon, J. ller,. B. urakami, J. Nagendra, H. amaswami, A. Humansettlements, infrastructure and spatial planning.Climate Change 2014:Mitigation of Climate Change. IPCC Working Group III Contribution toAR5; Cambridge University Press, 2014; Chapter 12.

Spokas, K.A., et al. 2021. Modeling landfill CH4 emissions: CALMIM international fieldvalidation, using CALMIM to simulate management strategies, current and futureclimate scenarios. Elem Sci Anth, 9: 1. https://doi.org/10.1525/elementa.2020.00050Do, 2020.

Tolaymat, T., M., R. B. Green, G. R. Hater, M. A. Barlaz, P. Black, D. Bronson, J. Powell, Evaluation of landfill gas decay constant for municipal solid waste landfills operated as bioreactors. J. Air Waste Manage. Assoc. 60, 91–97, 2010.

United States Environmental Protection Agency (USEPA), Global Mitigation of Non-CO_2 Greenhouse Gases 2010-2030 (United States Environmental Protection Agency Office of Atmospheric Programs (6207J), EPA-430-R-13-011, 2013); www.epa.gov/sites/production/files/2016-07/documents/mac_report_2014-exec_summ.compressed.pdf

Verhulst, K. R., Karion, A., Kim, J., Salameh, P. K., Keeling, R. F., Newman, S., Miller, J., Sloop, C., Pongetti, T., Rao, P., Wong, C., Hopkins, F. M., Yadav, V., Weiss, R. F., Duren, R. M. and Miller, C. E.: Carbon dioxide and methane measurements from the Los Angeles Megacity Carbon Project – Part 1: calibration, urban enhancements, and uncertainty 10 estimates, Atmos. Chem. Phys., 17(13), 8313–8341, doi:10.5194/acp-17-8313-2017, 2017

https://doi.org/10.5194/acp-2022-549
Preprint. Discussion started: 17 October 2022

Atmospheric Chemistry and Physics Discussions

Wang, X., A. S. Nagpure, J. F. DeCarolis, M. A. Barlaz, Characterization of uncertainty in estimation of methane collection from select U.S. landfills. Environ. Sci. Technol. 49, 1545–1551, 2015.

Wang, Y., Wang, X., Wang, K. *et al.* The size of the land carbon sink in China. *Nature*, E7–E9. https://doi.org/10.1038/s41586-021-04255-y, 2022.

Zhao, X., Jin, X., Guo, W., Zhang, C., Shan, Y., Du, M., Tillotson, M., Yang, H., Liao, X., and Li, Y.: China's urban methane emissions from municipal wastewater treatment plant, Earths Future, 7, 480–490, 2019.

Zhao, Z., Bian, R., Zhao, F., Chai, X., Implications of municipal solid waste disposal methods in China on greenhouse gas emissions. Renew. Sust. Energ. Rev. 39 (3). https://doi.org/10.1002/ep.13372, 2019.

Zhang, B. and Chen, G.: China's CH_4 and CO_2 emissions: Bottomup estimation and comparative analysis, Ecol. Indic., 47, 112– 122, https://doi.org/10.1016/j.ecolind.2014.01.022, 2014.

Zhang, K., Lee, X., Schultz, N. M., Huang, Q., Liu, Z., Chu, H., Zhao, L., & He, C. A global dataset on subgrid land surface climate (2015-2100) from the Community Earth System Model. Geosci. Data J., 1–12. https://doi.org/10.1002/gdj3.153, 2022.

https://doi.org/10.5194/acp-2022-549
Preprint. Discussion started: 17 October 2022

Atmospheric Chemistry and Physics Discussions

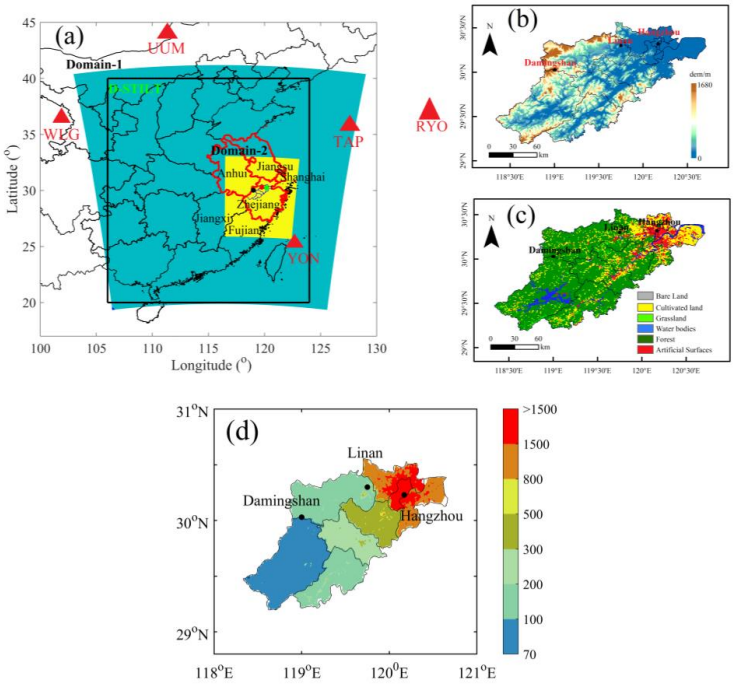

Figure 1. (a) WRF-STILT model domain setup, three CH_4 concentration observation sites in Hangzhou city, and five CH_4 background sites. Note that the green, red and black dots represent the locations for the Hangzhou, Linan and Damingshan sites, respectively. The Yangtze River Delta region is contained in the red boundary, and the back rectangle represents domain in STILT model. (b) Geophysical height within Hangzhou city, (c) land surface categories in Hangzhou city, and (d) population density in Hangzhou city for 2019, units: person per km^2.

https://doi.org/10.5194/acp-2022-549
Preprint. Discussion started: 17 October 2022

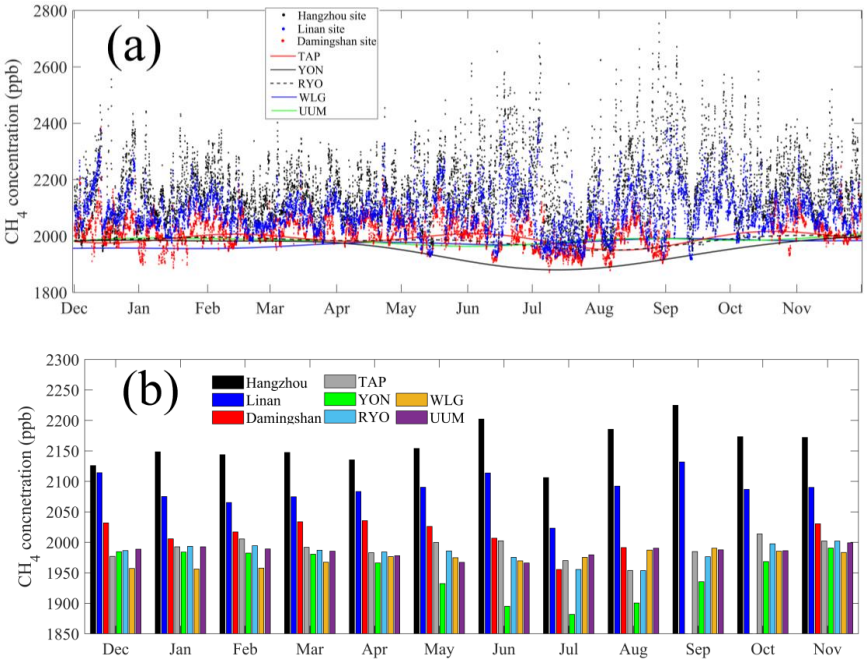

Figure 2. (a) Hourly CH_4 concentrations at three sites within Hangzhou city, namely, Hangzhou site, Linan site, and Damingshan site, and CH_4 background fit based on the CCGCRV regression method at five background sites, namely, TAP, YON, RYO, WLG, and UUM; and (b) monthly mean CH_4 concentrations for the above eight sites. Note that the CH_4 background is smoothed by using the CCGCRV fitting method based on weekly or hourly observations, which can filter large fluctuations caused by sudden and unidentified sources

https://doi.org/10.5194/acp-2022-549
Preprint. Discussion started: 17 October 2022

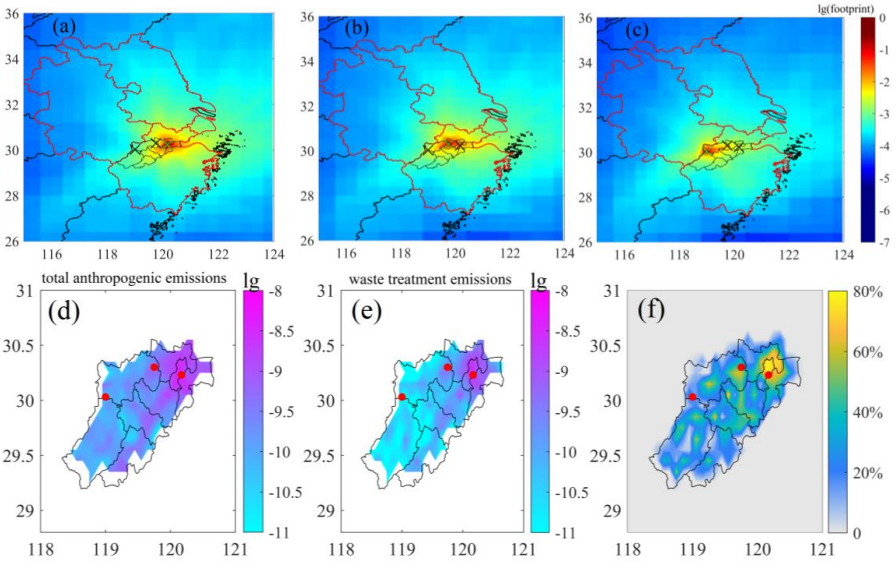

Figure 3. Annual averages of the simulated footprint for the (a) Hangzhou site, (b) Linan site, and (c) Damingshan site, where the green symbol "×" indicates the receptor location in each panel, (d) total anthropogenic CH_4 emissions according to the EDGAR v6.0 inventory, (e) waste treatment CH_4 emissions, and (f) proportion of waste treatment emissions to total anthropogenic CH_4 emissions. The red dot represents three sites, the unit for the footprint is ppm m^2 s mol^{-1}, and the unit for emissions is kg m^{-2} s^{-1}.

https://doi.org/10.5194/acp-2022-549
Preprint. Discussion started: 17 October 2022

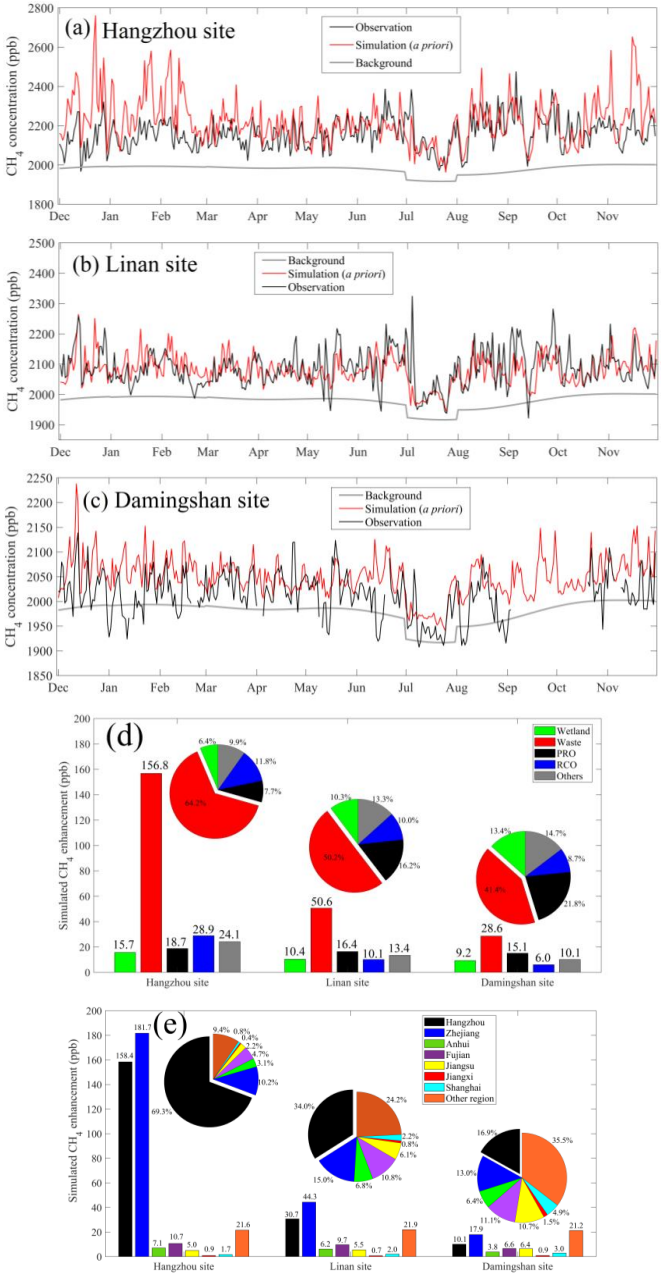

Figure 4. Comparisons between daily CH_4 observations and simulations for the (a) Hangzhou site, (b) Linan site, (c) Damingshan site, (d) simulated CH_4 enhancements from main emission categories, and (e) simulated anthropogenic CH_4 enhancement from different regions and proportions. Note that contributions from Zhejiang Province in the pie figure (e)represent the sum of both "Hangzhou" and "Zhejiang".

https://doi.org/10.5194/acp-2022-549
Preprint. Discussion started: 17 October 2022

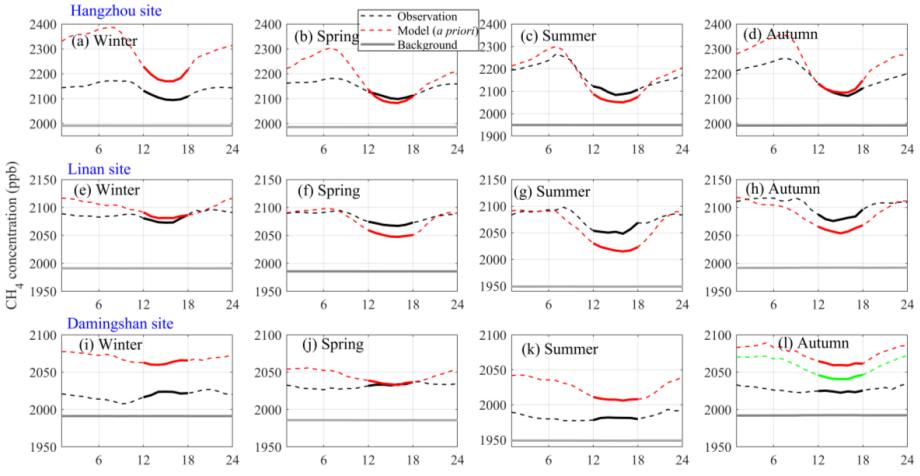

Figure 5. Seasonal averaged diurnal variations for the Hangzhou site in (a) winter, (b) spring, (c) summer, and (d) autumn; Linan site in (e) winter, (f) spring, (g) summer, and (h) autumn; and Damingshan site in (i) winter, (j) spring, (k) summer, and (l) autumn; Note, because of the two-months data gap in autumn for the Damingshan site, the green line is for all September-November simulations, the red line only represents simulations for the corresponding period for available observation data, and the bold lines represent data between 12:00 and 18:00.

https://doi.org/10.5194/acp-2022-549
Preprint. Discussion started: 17 October 2022

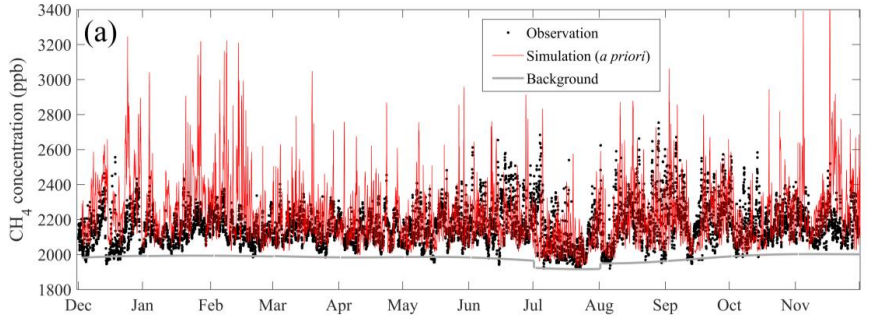

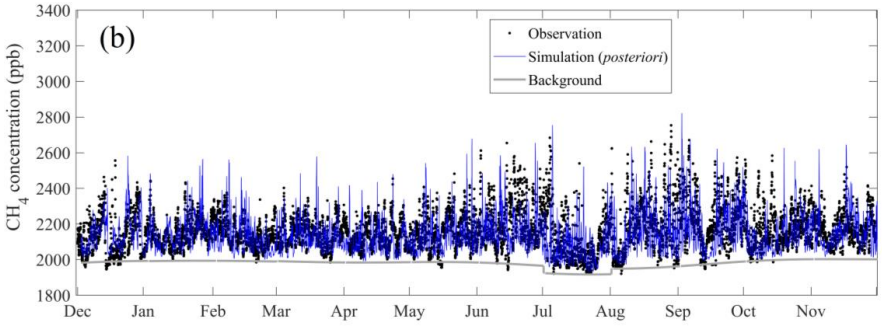

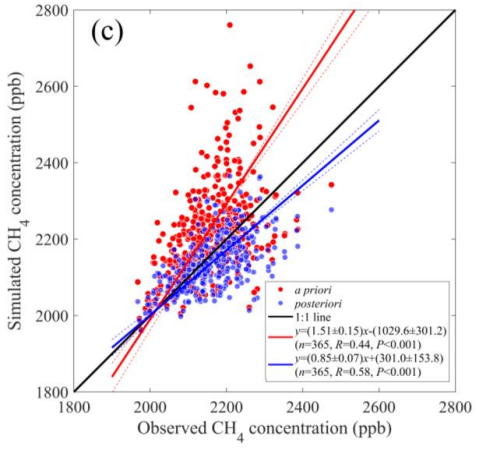

Figure 6. Comparisons of the hourly CH_4 concentrations at the Hangzhou site between observations and simulations by using (a) *a priori* and (b) *posteriori* emissions and (c) scatter plots of daily CH_4 averages by using *a priori* and *posteriori* emissions.

https://doi.org/10.5194/acp-2022-549
Preprint. Discussion started: 17 October 2022

Atmospheric Chemistry and Physics Discussions

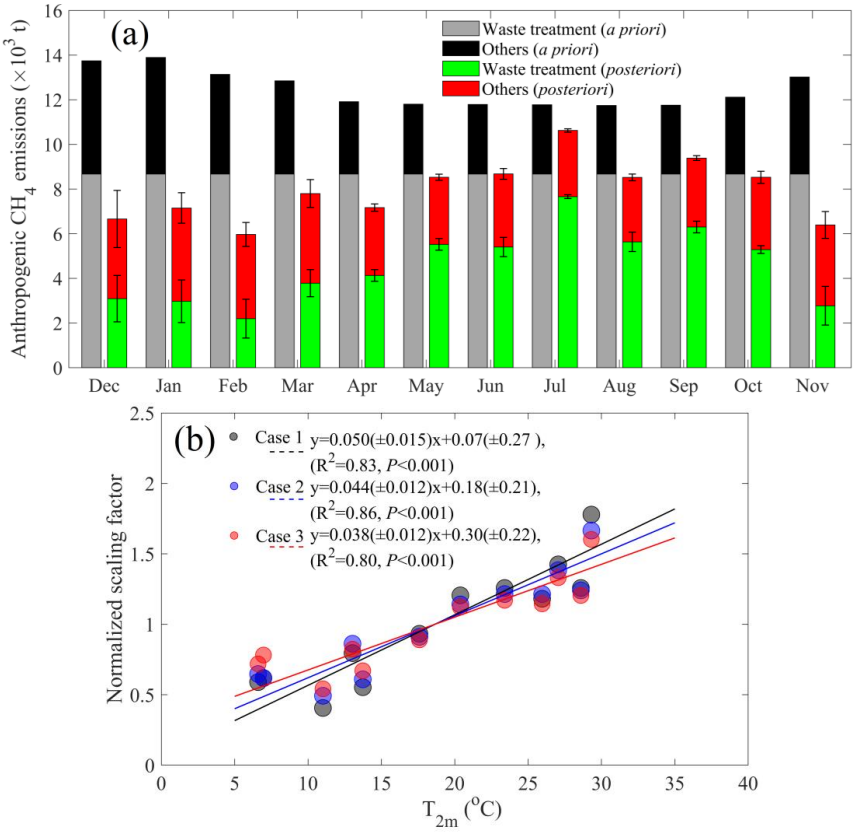

Figure 7. (a) Monthly anthropogenic (excluding agricultural soil) CH_4 emissions for *a priori* and *posteriori* emissions for Hangzhou city and (b) relationship between the monthly *posteriori* CH_4 emissions and temperature in three cases.

https://doi.org/10.5194/acp-2022-549
Preprint. Discussion started: 17 October 2022

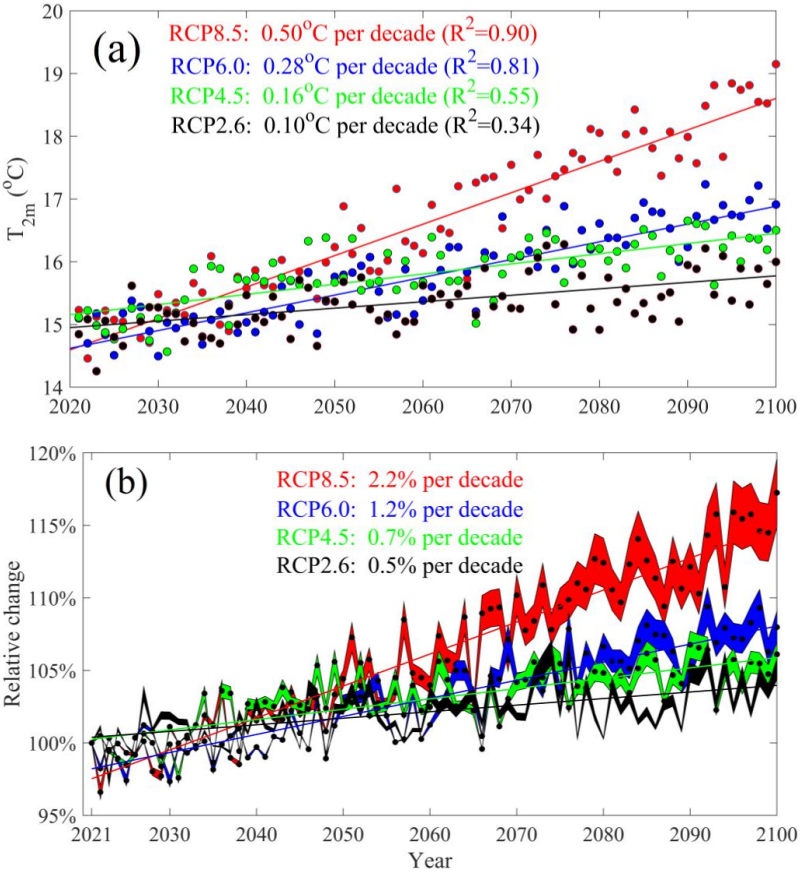

Figure 8. (a) Annual air temperature from 2021 to 2100 for the four different global warming scenarios and, (b) projected relative change of waste treatment CH_4 emissions (or EFs). Note that the shading indicates the extent of three cases.

https://doi.org/10.5194/acp-2022-549
Preprint. Discussion started: 17 October 2022

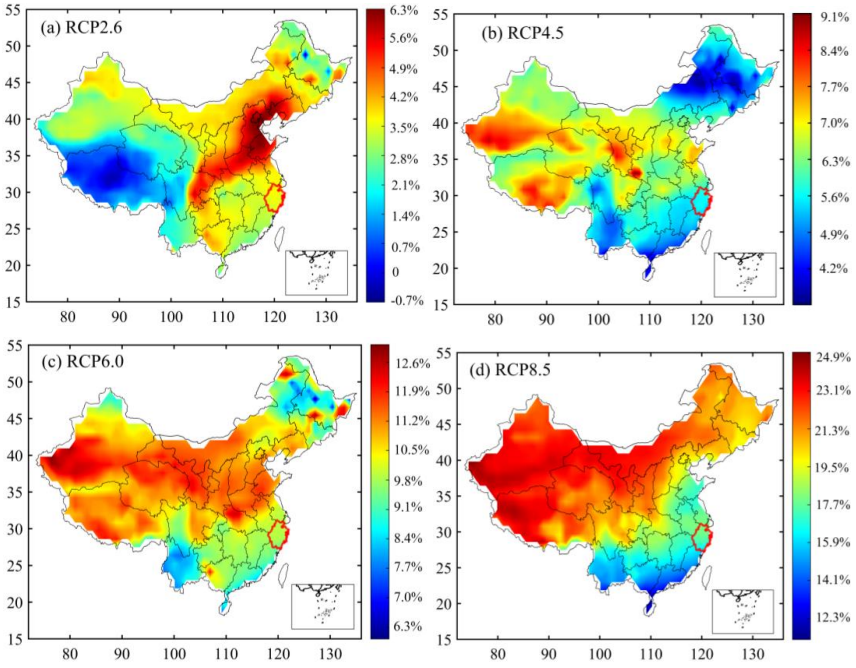

Figure 9. Global warming-induced relative changes of the waste treatment CH_4 EFs by year for 2100 for the (a) RCP2.6, (b) RCP4.5, (c) RCP6.0, and (d) RCP8.5 scenarios. Note that the red boundary is Zhejiang Province.

https://doi.org/10.5194/acp-2022-549
Preprint. Discussion started: 17 October 2022

Atmospheric Chemistry and Physics Discussions

Table 1. *Posteriori* SFs for different categories in three cases, where wetland represents natural and agricultural wetland, Waste represents waste treatment, PRO represents fuel exploitation, RCO represents energy for building, and Others represents the remaining anthropogenic emissions.

	Case 1			Case 2					Case 3		
Month	Wetland	Waste	Others	Wetland	Waste	PRO	RCO	Others	Wetland	Waste	Others
1	1.00	0.29	0.83	1.00	0.34	0.90	0.80	0.93	1.00	0.40	0.72
2	1.00	0.20	0.89	1.00	0.26	0.97	0.83	0.93	1.00	0.30	0.77
3	1.03	0.39	1.04	1.02	0.46	1.07	0.80	0.97	1.02	0.46	0.95
4	1.10	0.46	0.96	1.08	0.48	1.01	0.95	0.93	1.08	0.49	0.91
5	1.12	0.62	0.99	1.10	0.64	1.06	0.97	0.92	1.11	0.65	0.95
6	1.22	0.59	1.09	1.18	0.64	1.05	0.97	1.03	1.18	0.64	1.05
7	1.10	0.88	0.96	1.09	0.88	1.00	1.00	0.94	1.09	0.89	0.94
8	1.05	0.62	0.95	1.01	0.66	0.99	0.97	0.95	1.01	0.67	0.91
9	1.04	0.71	1.01	1.02	0.73	0.96	0.98	1.04	1.02	0.74	0.98
10	1.06	0.60	0.94	1.06	0.61	0.92	0.96	1.00	1.06	0.62	0.90
11	1.01	0.27	0.86	1.00	0.32	0.91	0.85	0.93	1.00	0.37	0.75
12	1.00	0.31	0.70	1.00	0.33	0.75	0.79	0.91	1.00	0.43	0.58